A compact highly sensitive refractive index sensor using a butterfly-shaped absorber for terahertz biomedical applications

GEETIKA*, R. S. KALER
Department of Electronics and Communication Engineering, Thapar Institute of Engineering and Technology, Patiala-147004, Punjab, India

In this work, the design and analysis of a butterfly-shaped perfect absorber is presented for Terahertz applications. The proposed absorber has compact dimensions of 16×16 μm^2. It comprises three layers, a butterfly-shaped metallic patch on the uppermost layer, a middle layer of Teflon and a metallic ground plane at the bottom. The perfect narrow absorption peak is observed at 4.7 THz with an absorption value of 99%. The design exhibits a fourfold symmetry with a tolerance of 60º for an angle of incidence and is polarisation insensitive. Further, the designed butterfly-shaped absorber is used to sense the analyte with a refractive index ranging from 1 to 3.16 exhibiting an average sensitivity value of 786 GHz/RIU for fixed analyte thickness. The compact and unique design of the sensor enhances its sensing performance, indicating its potential for various applications such as biomedical sensing, hazardous substance detection, and disease diagnosis.

(Received March 13, 2024; accepted October 2, 2024)

Keywords: Metamaterial, THz sensors, Sensitivity, Polarization and absorber

1. Introduction

In recent times, terahertz (THz) radiation for the sensing phenomenon has captivated researcher's attention due to the properties of infrared and microwave frequency bands. Because of the limited accessibility of THz-producing sources and detectors, there has been restricted research in this band. Therefore, effective devices in this band have become an important topic of study and several researchers are now exploring terahertz technology [1]. Terahertz-based absorbers are now grabbing attention in the present years due to their applications in communication [2], sensing [3], imaging [4] and material characterization [5]. So, various medical applications are using THz technology due to the non-ionizing and non-invasive characteristics of THz waves. Metamaterials are subwavelength-based artificial materials having a negative dielectric constant and refractive index (RI) that cannot be realized by naturally existing materials. Researchers have observed that incident radiation can be strongly absorbed by metamaterials at the frequency of resonance [6]. So, the metamaterial-based absorber study has become an important topic in the THz regime. The typical configuration of a Terahertz metamaterial absorber (TMA) comprises an uppermost layer of a frequency-selective structural array, a dielectric substrate in the middle layer, and a lower metallic plane to prevent electromagnetic wave transmission. The metallic pattern is designed to attain maximum absorption of the incoming wave. The first THz absorber was described in 2008 with 70% absorptivity at 1.3 GHz [7]. By varying the permeability and permittivity of the structure, absorption with maximum value can be achieved through resistive and dielectric losses due to the reduction in transmissivity and reflectivity simultaneously at the resonant frequency. Since then, various metamaterial-based absorbers have been studied by researchers having different bands of absorption including narrowband [8], multiband [9], broadband [10] and ultrabroad band [11]. The bandwidth of absorption is the most significant factor in the various applications. Narrowband absorbers include thermal emitters [12] and sensors [13]. Broadband absorbers are mostly used in photodetectors [14] and solar cells [15] whereas multi-band absorbers are used in multispectral imaging [16] and sensing [17]. Also, the absorption spectra obtained can differ by the variations in the surrounding environment. Hence, variations in the spectra can be used to identify the factor responsible for the shift, making these structures valuable as sensing devices. TMAs find common applications in refractive index-based sensing, temperature sensing, biomedical sensing etc. [18].

Terahertz absorber sensors are often preferred over plasmonic sensors due to their distinct advantages in various applications, such as non-destructive imaging, material analysis, and spectroscopy [19-20]. These sensors excel in deeper penetration into materials, allowing them to investigate internal structures and compositions without causing damage, over plasmonic sensors limited to surface-level measurements due to their operation in the visible to near-infrared ranges [21-23]. Additionally, the fabrication of THz absorber sensors is straightforward and cost-effective compared to plasmonic sensors, which require complex nanostructures and sophisticated techniques, increasing cost and complicating scalability [24-25].

The research focuses on the unique design of such a sensor to detect various materials. The materials are detected concerning the change in the resonant peak of the sensor when a sample is loaded on it. The absorption, reflection and transmission characteristics are measured to evaluate the sensor's performance. In [26], a terahertz sensor of size 96 × 96 μm^2 with a dual-band based on a perfect metamaterial absorber having 638 GHz/RIU sensitivity using a double-ring metal microstructure array was studied. Sabah et al. [27] designed a TMA-based sensor having a cross-like structure with a 7.66 GHz/μm sensitivity. THz biomedical sensor using split ring resonators of dimension $0.391\lambda_{eff} \times 0.391\lambda_{eff}$, having a resonant frequency of 2.249 THz, is presented in [28] with 300 GHz/RIU sensitivity for detecting blood components. Many of these sensors have sensitivities that still cannot meet the demands of many practical applications.

This paper presents a compact THz metamaterial-based perfect absorber designed to sense changes in the refractive index of an analyte. The structure presented here differs from existing metamaterial RI sensors in the literature. The design is comparatively simple and consists of two orthogonal elliptical ring resonators with slots in them to obtain maximum absorptivity. The average absorptivity calculated for the sensor is 99%. The theoretical RI values have been used for the sensitivity calculation. The RI sensitivity of 786 GHz/RIU is obtained whereas thickness sensitivity is 245 GHz/μm respectively. The proposed structure features a butterfly-shaped metallic patch and a compact size, resulting in a highly efficient absorber with superior performance in absorption and sensitivity compared to conventional designs. The unique shape provides distinct resonant properties that enhance the sensor's performance, while the compact design minimizes the overall footprint without compromising performance. In Section 2, the design and evolution process is described. The stability analysis, parametric variations and sensitivity of the proposed absorber are investigated in Section 3. Finally, Section 4 concludes the paper.

2. Design configuration and its evolution

The proposed design of a butterfly-shaped absorber utilizing THz metamaterial is depicted in Fig. 1. The 3-D view and top view of the unit cell are given in Fig. 1(a) and (b) respectively. The size obtained after optimization for the suggested structure is 16 × 16 μm^2. The basic idea for this geometry has been inspired by a metamaterial absorber, incorporating metal-dielectric-metal layers in the design. The geometry comprises a metallic resonator layer of gold at the uppermost layer, a middle layer of polytetrafluoroethylene (Teflon) used as a substrate having a permittivity value of 2.1, the loss tangent of 0.01 and a complete gold-based metallic ground plane at the back as shown in Fig. 1(c). The two orthogonal elliptical ring resonators are placed at 45º with respect to the metallic ground plane axis having major radius r_1 and minor radius r_2 with slots radii r_3 and r_4 respectively. The elliptical ring resonator is composed of gold, which possesses a conductivity value of 4.6 × 10^7 S/m, acting as the top layer to be used as a frequency-selective surface.

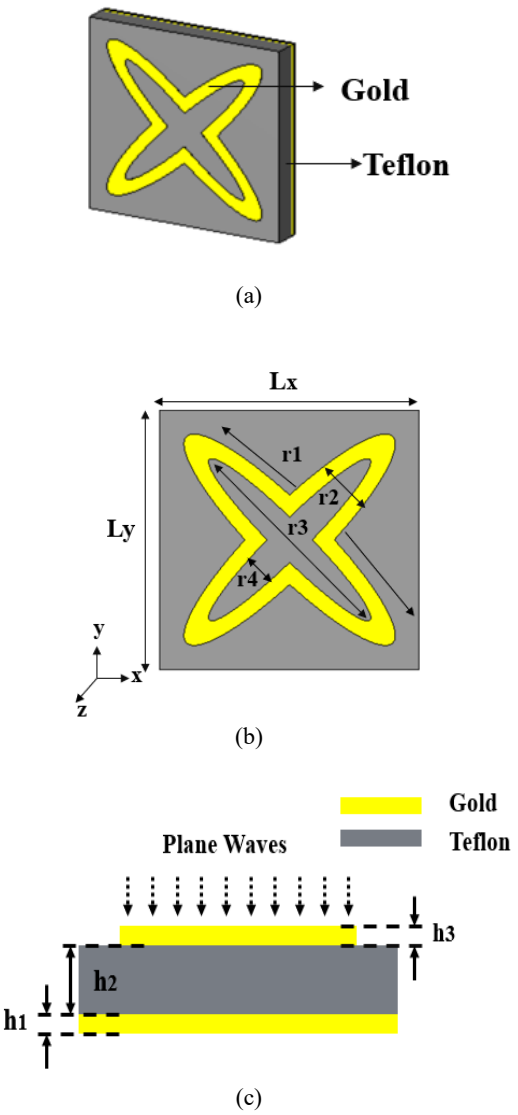

Fig. 1. Proposed absorber unit cell from three different perspectives: (a) 3-D view, (b) top view, and (c) side view (color online)

The process of evolution for the proposed butterfly-shaped absorber is discussed in detail in this section. At the initial stage, two elliptical ring resonators, oriented orthogonal to each other, are printed on the substrate layer and then rotated from the x-y plane at an angle of 45º, as shown in Fig. 2(a). The result obtained after simulation from the initial stage is illustrated in Fig. 2(c) having a resonant frequency of 6.3 THz with an absorption value of 53%. To attain the desired results at a lower resonance frequency without enlarging the absorber's dimensions, two elliptical slots of radii r_3 and r_4 have been etched from the design in the final stage as portrayed in Fig. 2(b) and their characteristics of absorption are given in Fig. 2(c). This etching helps in obtaining the absorption of 99% as well as lowering the resonant value of frequency from 6.3

THz to 4.7 THz. The final geometry of the proposed structure is shaped like a butterfly-shaped absorber. The geometrical parameters of the butterfly absorber have been optimized effectively to align the absorber impedance with the impedance of free space for achieving maximum absorption. The parameters obtained after optimization have been tabulated in Table 1. Also, reflection, absorption and transmission characteristics are plotted in Fig. 3. It is evident that the designed structure exhibits zero transmission due to metallic ground plane, minimal reflection, and high absorption at a frequency of 4.7 THz.

Table 1. Optimized dimensions of butterfly-shaped absorber

Parameters	L	h_1	h_2	h_3	r_1	r_2	r_3	r_4
Values (μm)	16	0.25	2	0.003	9	2	7	1

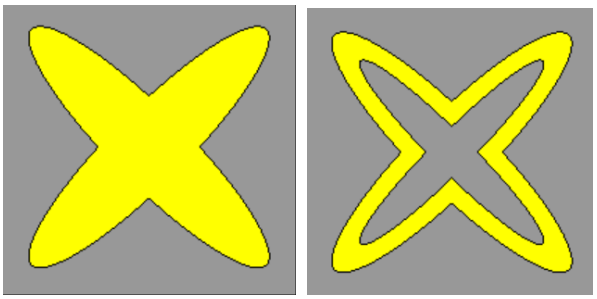

(a) (b)

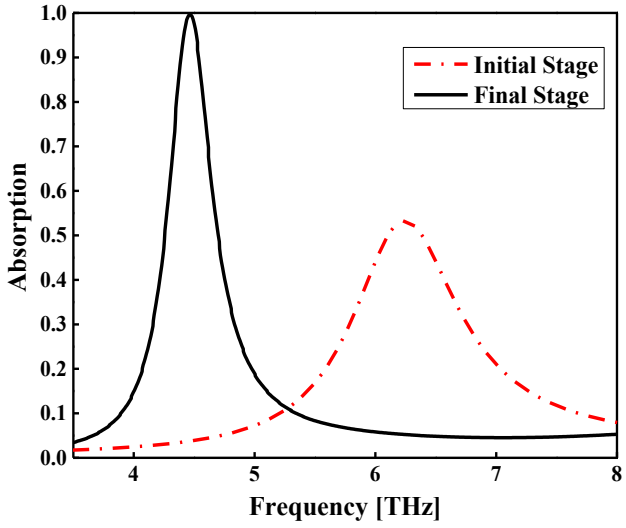

(c)

Fig. 2. (a) Initial Stage (b) Final Stage and (c) Absorption characteristics of an evolution process (color online)

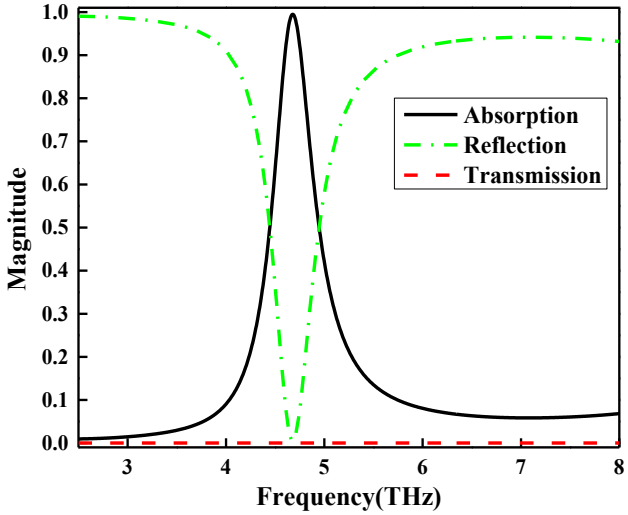

Fig. 3. Absorption, reflection and transmission characteristics of proposed butterfly absorber (color online)

3. Results and discussion

The simulations of the proposed butterfly-shaped perfect absorber have been performed using the Computer Simulation tool (CST) studio suite by applying adaptive tetrahedral mesh. The absorption characteristics are studied using the technique of finite integration by applying periodic boundary conditions along the x and y-axis, and the boundary condition of the floquet port in the z-axis. An input EM wave is propagating in the z direction and can be transverse electric or transverse magnetic. The absorption properties of the proposed butterfly-shaped absorber are obtained from the scattering parameters. The mathematical equation used for calculating the value of absorption is given as [24].

$$A(\omega) = 1 - R(\omega) - T(\omega) = 1 - |S_{11}|^2 - |S_{21}|^2 \quad (1)$$

where A is the absorption rate, T denotes the transmission rate and R is the reflection rate. Here S_{11} indicates the coefficient of reflection and S_{21} indicates the coefficient of transmission.

The bottom layer is taken to be completely metallic for blocking the transmission of the incident wave (S_{21}=0). Thus, the absorption equation is given as [24].

$$A(\omega) = 1 - R(\omega) = 1 - |S_{11}|^2 \quad (2)$$

The main aim is to achieve higher absorption by reducing reflection since transmission is zero. According to the transmission line theory [25], reflection becomes zero after the input impedance aligns completely with the impedance of free space. The value of input impedance is given as

$$Z = (1 + S_{11})/(1 - S_{11}) \quad (3)$$

The surface current distribution, electric and magnetic field are presented to explain the absorption mechanism in

more detail. Fig. 4(a) shows the distribution of current along the surface of the x–y plane, and Fig. 4(b), and (c) show the electric field and magnetic field at the absorption frequency of 4.7 THz respectively. As shown, the electric as well as magnetic fields are intense mostly on the four outer edges of the ring, representing strong electrical as well as magnetic resonances

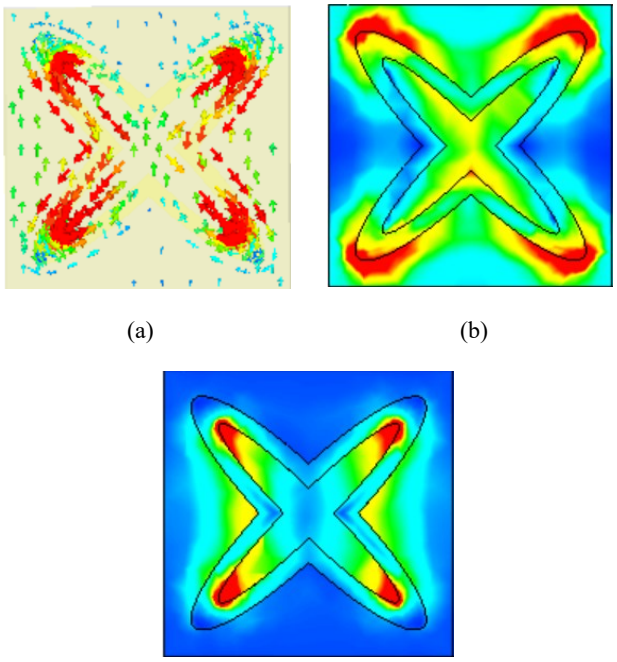

(a) (b)

(c)

Fig. 4. (a) Surface current distribution (b) E-field and (c) H-field at a resonant frequency of 4.7 THz (color online)

3.1. Parametric variation

The effect of variation of some crucial parameters of the proposed butterfly absorber on absorption has been investigated in this section.

- **Effect of height of substrate (h_2)**

An optimal height is important for achieving the desired absorption peak at a specific frequency, as it affects the fundamental resonant properties and wave interactions of the absorber. As shown below in Fig. 5, the substrate height (h_2) ranges from 1.5 to 2.5 µm having an increment of 0.5 µm. The optimal height of the substrate is 2 µm due to the fact that any deviation, whether increasing or decreasing the dimensions from the optimized value, results in a reduction of the absorption value.

- **Effect of slot width (r2)**

The width of slot (r2) is varied from 5 to 9 µm having an increment of 2 µm as illustrated in Fig. 6. The optimal value of r2 is obtained at 7 µm due to the high absorption value as plotted in figure below:

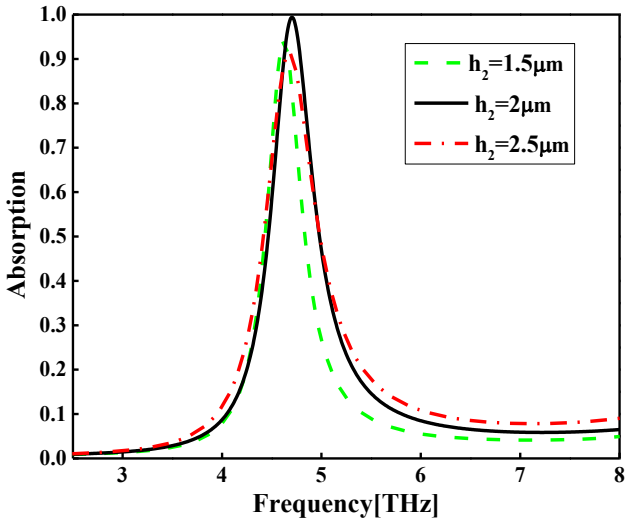

Fig. 5. Impact on absorption value with variation in substrate height 'h_2' (color online)

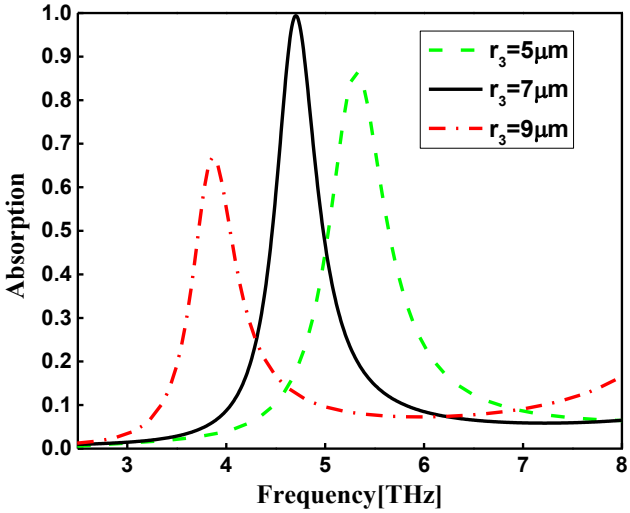

Fig. 6. Impact on absorption value with variation in slot 'r_3' (color online)

3.2. Stability analysis

The absorber's aim is not solely to attain maximum absorption with a narrow bandwidth but also to preserve a simple and symmetrical structure, as it ensures insensitivity to variations in polarization angles. In this section, polarization as well as angular stability analysis for the proposed butterfly-shaped absorber has been presented. The EM wave is incident on the absorber in the z-axis.

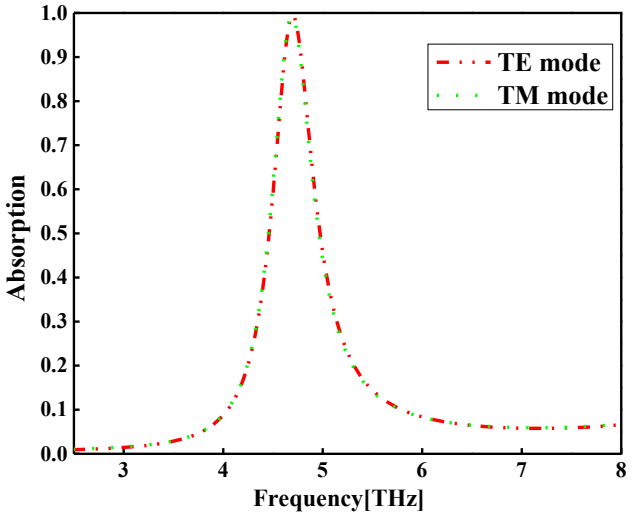

Fig. 7. Absorption characteristics for polarization independency (color online)

The polarization independency of the absorber is evaluated using the condition of normal incidence (θ = 0º) for transverse electric and transverse magnetic modes, respectively. The symmetrical behaviour of the proposed absorber ensures identical characteristics for TE as well as TM modes as portrayed in Fig. 7. Thus, the designed absorber demonstrates polarization-insensitive behaviour within the THz spectrum

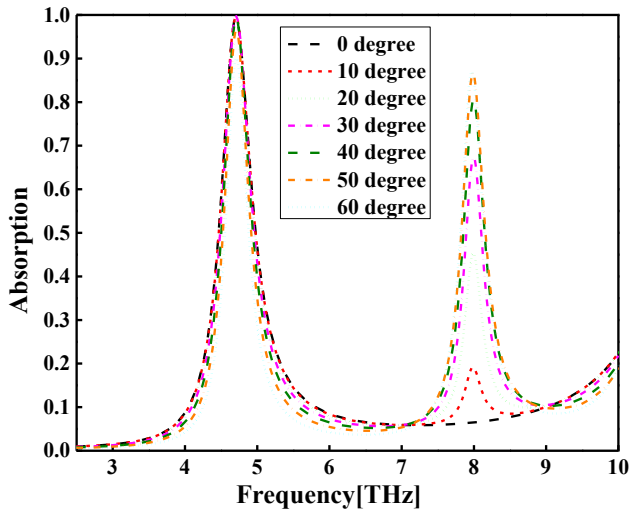

Fig. 8. Absorption characteristics for different angles of incident (color online)

Furthermore, the absorption value is studied for an angle of incidence θ ranging from 0º to 60º and its absorption spectra are displayed in Fig. 8. The graph helps to determine the maximum angular stability at θ=60°. Since the oblique incidence values for TE, as well as TM modes, are nearly equal, the designed geometry exhibits polarisation-independency. The results achieved for a wide range of incident angles are considerably satisfactory. Also, new peaks are simultaneously generated at a higher angle of incidence due to the higher modes generation inside the dielectric at a lower wavelength value as given in Fig. 9. It is demonstrated from the above-given results that the proposed butterfly-shaped absorber is independent of polarization and angularly stable for angle of incidence θ up to 60º.

3.3. Sensing performance

In this section, we have explored the utilization of the desired absorber in sensing applications. The evaluation of sensing performance is done by loading sample material of an analyte at the upper layer of the proposed design as shown in Fig. 9. To obtain sensing characteristics, the RI of an analyte is varied from 1.41 to 3.16 (ε_r =2 to 10) at a constant analyte thickness of 1μm and important parameters such as sensitivity and Q factor is examined. The sensitivity formula is given by

$$S = \Delta f/\Delta n \text{ (GHz/RIU)} \quad (4)$$

where Δf is the shift in resonant frequency peak, Δn denotes the variation in refractive index. The plot of absorptivity and deviation in the frequency is shown in Fig. 10. The redshift (left side) in resonant frequency is obtained by increasing the value of the dielectric constant due to the change in the total capacitance of the design. The capacitance of the designed structure increases with the accumulation of an analyte layer [26] and therefore, the resonant frequency shifts downwards. Thus, the sensor exhibits an average sensitivity of 786 GHz/RIU for RI values from 1.41 to 3.16. Hence, the sensor is extremely sensitive to RI variation as shown in Fig. 10.

Table 2 presents the metrics for the proposed butterfly-shaped refractive index sensor. The table indicates that sensitivity decreases as the refractive index increases whereas Table 3 provides a performance comparison between the proposed sensor and other sensors reported in the literature.

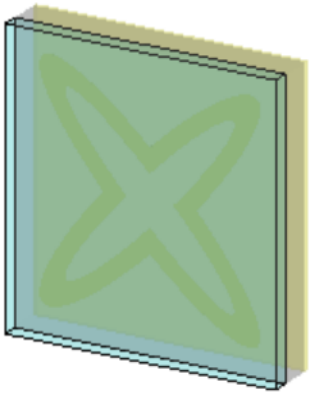

Fig. 9. Setup used for estimation of sensitivity (color online)

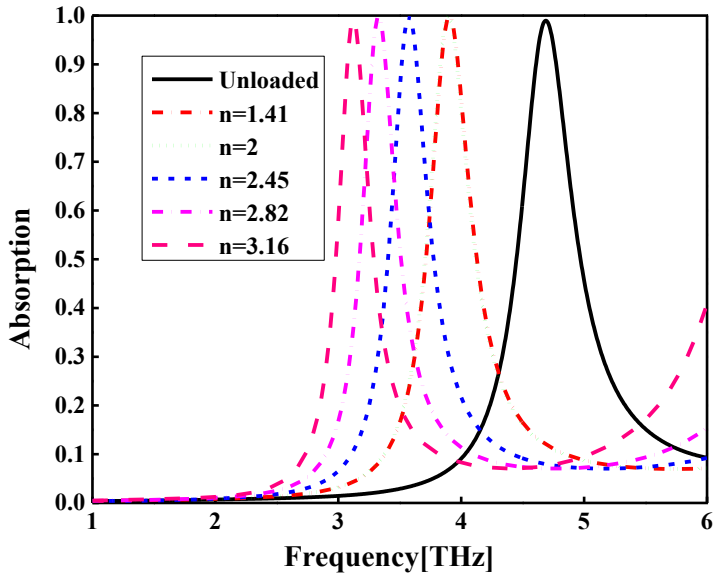

Fig. 10. Absorption characteristics for various materials (color online)

Table 2. Absorption characteristics for various refractive index

Refractive Index	Absorption (%)	Resonant Frequency (THz)	S(GHz/RIU)	FWHM (GHz)	Q	FOM
1	98	4.7		600	7.83	
1.41	99	4.34	878	500	8.68	1.756
2	98	3.9	800	430	9.06	1.86
2.45	98	3.6	758	400	9	1.9
2.82	98	3.31	764	400	8.3	1.91
3.16	98	3.13	727	400	7.8	1.82

Table 3. Performance of proposed design compared to those mentioned in the literature

Ref.	Detection Purpose	Size (µm x µm)	Resonance Frequency	Sensitivity	Absorptivity	FOM
[26]	RI ranges from 1 to 2.1 with 5 µm analyte thickness	96 × 96	1.77THz	638 GHz/ RIU	99%	-
[27]	Dielectric variation of 1 to 15 with an analyte thickness of 1 µm	300 ×300	1.67THz	7.66GHz/ µm	99.9%	1.5
[28]	Thickness deviation from 1 to 8 µm with 1.35 RI	36×36	2.145 THz	23.7 GHz/ µm	98%	0.23
[29]	Dielectric variation of 1 to 5 with thickness of 1 µm	50 × 50	4.4754 THz	22.75GHz/RIU	98.88%	0.48
[30]	Thickness range from 0 to 6 µm, 6 to 16 µm with fixed n=1.6	110×110	0.533 THz	6.27GHz/ µm	98.8%	0.418
This work	RI from 1 to 3.9 with an analyte thickness of 1 µm	16 ×16	4.17 THz	786GHz/RIU	99%	1.9

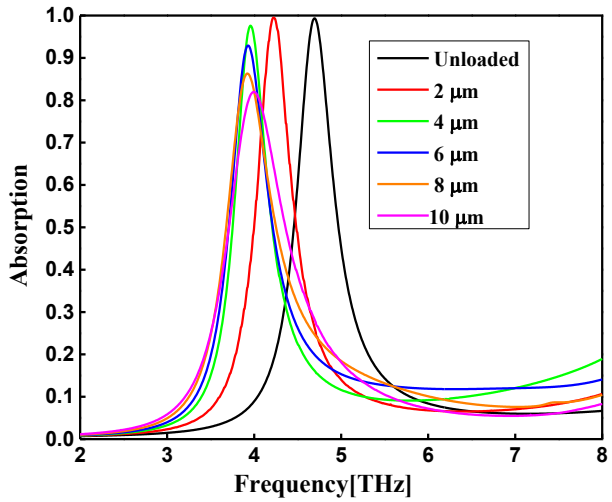

Fig. 11. Absorption characteristics for various analyte thickness (color online)

Similarly, the thickness sensitivity is evaluated at fixed RI at 1.6 by varying the thickness of the analyte from 1 to 10 µm. The estimated average frequency deviation of 245 GHz/µm is obtained. The shift in resonant frequency with variation in analyte thickness is given in Fig. 11. As a result, even slight variations in the analyte's thickness or RI can bring a noticeable shift in the resonance frequency of the MPA, rendering it suitable for sensor application.

4. Conclusion

In this work, a compact butterfly-shaped perfect absorber is designed for terahertz applications. The design is made up of two elliptical ring resonators placed orthogonally to each other to obtain the maximum absorption of 99% at 4.7 THz. Also, this THz absorber is polarisation insensitive and angularly stable up to 60º, making it practically viable for healthcare, applications. The proposed absorber exhibits a high sensitivity of 786 GHz/ RIU obtained by varying the analyte's refractive index ranging from 1 to 3.16 at 1 µm thickness. Moreover, the thickness sensitivity of 245 GHz/um is obtained by changing the thickness value of the analyte layer from 1 µm to 10 µm at a fixed refractive index. This sensor can bring a revolutionary change in the field of biomedical applications due to less complex design with better sensitivity.

Competing interests

The authors declare that they have no known conflicts of interest associated with this publication.

Author's Contribution

All authors contributed to the study's conception and design. All authors read and approved the final manuscript.

Funding

The authors declare that no funds, grants, or other support were received during the preparation of this manuscript.

Data Availability

Data sharing is not applicable to this article as no datasets were generated or analysed during the current study.

References

[1] D. W. Porterfieldin, IEEE/MTT-S International Microwave Symposium, Honolulu, HI, USA, **337** (2007).
[2] K. S. Bhatia, R. S. Kaler, T. S. Kamal, R. Randhawa, Optik **124**(2), 117 (2013).
[3] J. M. Jornet, I. F. Akyildiz, IEEE Journal on Selected Areas in Communications **31**(12), 685 (2013).
[4] R. S. Kaler, T. S. Kamal, A. K. Sharma, S. K. Arya, R. Agarwala, Fiber and Integrated Optics **21**(3), 193 (2002).
[5] Z. Wang, Y. Han, N. Xu, L. Chen, C. Li, L. Wu, W. Zhang, IEEE Transactions on Terahertz Science and Technology **8**(2), 161 (2018).
[6] C. M. Watts, X. Liu, W. J. Padilla, Advanced Optical Materials **24**(23), 98 (2012).
[7] H. Tao, N. I. Landy, C. M. Bingham, X. Zhang, R. D. Averitt, W. J. Padilla, Optics Express **16**(10), 7181 (2008).
[8] L. Shi, J. Shang, Z. Liu, Y. Li, G. Fu, X. Liu, P. Pan, H. Luo, G. Liu, Nanotechnology **31**(46), 1 (2020).
[9] Y. He, Q. Wu, S. Yan, Plasmonics **14**(6), 1303 (2019).
[10] J. Huang, J. Li, Y. Yang, J. Li, J. Li, Y. Zhang, J. Yao, Optics Express **28**(12), 17832 (2020).
[11] A. Fardoost, F. G. Vanani, A. Amirhosseini R. Safan, IEEE Transactions on Nanotechnology **16**(1), 68 (2017).
[12] M. Diem, T. Koschny, C. M. Soukoulis, Physical Review B **79**, 033101 (2009).
[13] N. Liu, M. Mesch, T. Weiss, M. Hentschel, H. Giessen, Nano Letters **10**(7), 2342 (2010).
[14] M. Mittendorf, S. Winnerl, J. Kamann, J. Eroms, D. Weiss, H. Schneider, M. Helm, Applied Physics Letters **103**(2), 02113 (2013).
[15] J. Li, X. Chen, Z. Yi, H. Yang, Y. Tang, Y. Yi, W. Yao, J. Wang, Y. Yi, Materials Today Energy **16**, 100390 (2020).
[16] Z. Zhou, T. Zhou, S. Zhang, Z. Shi, Y. Chen, W. Wan, X. Li, X. Chen, S. N. G. Corder, Z. Fu, L. Chen, Y. Mao, J. Cao, F. G. Omenetto, M. Liu, H. Li, T. H. Tao, Advanced Science **5**(7), 1700982 (2018).
[17] B. X. Wang, X. Zhai, G. Z. Wang, W. Q. Huang, L. L. Wang, Journal of Applied Physics **117**(1), 014504 (2014).

[18] W. Xu, X. Lijuan, Y. Ying, Nanoscale **9**(37), 13864 (2017).
[19] S. Khani, M. Hayati, Superlattices and Microstructures **156**, 106970 (2021).
[20] M. A. Butt, N. L. Kazanskiy, S. N. Khonina, Measurement **211**, 112601 (2023).
[21] S. Khani, M. Hayati, Scientific Reports **12**(1), 5246 (2022).
[22] S. B. Saadatmand, M. J. H. N. Chemerkouh, V. Ahmadi, S. M. Hamidi, Journal of the Optical Society of America B **40**(1), 1 (2023).
[23] S. M. Ebadi, S. Khani, Plasmonics **18**(4), 1607 (2023).
[24] M. A Haque, R. Rahad, A. K. M. Rakib, S. Sharar, R. H. Sagor, Results in Physics **51**, 106733 (2023).
[25] X. Zhu, Z. Qian, X. Chen, L. Liu, C. Sheng, W. Gu, IEEE Sensors Journal **21**(5), 5836 (2021).
[26] W. Zhang, F. Lan, J. Xuan, P. Mazumder, M. Aghadjani, Z. Yang Proceedings IEEE MTT-S International Microwave Workshop Series on Advanced Materials and Processes for RF and THz Applications (IMWS-AMP), 1 (2017).
[27] C. Sabah, B. Mulla, H. Altan, L. Ozyuzer, Pramana **91**(2), 17 (2018).
[28] A. S. Saadeldin, M. F. O. Hameed, E. M. A. Elkaramany, S. S. A. Obayya, IEEE Sensors Journal **19**(18), 7993 (2019).
[29] A. Veeraselvam, G. N. A. Mohammed, K. Savarimuthu, J. Anguera, J. C. Paul, R. K. Krishnan, Sensors **21**(23), 8151 (2021).
[30] Z. Xiong, L. Shang, J. Yang, L. Chen, J. Guo, Q. Liu, S. A. Danso, G. Li, IEEE Access **9**, 59211 (2021).

*Corresponding author: gmehandiratta_phd18@thapar.edu